Check for updates

View Article Online
View Journal

Dalton Transactions

Accepted Manuscript

This article can be cited before page numbers have been issued, to do this please use: Y. Yang, H. Huang, Y. Wang, F. Qiu, Y. Feng, X. Song, X. Tang, G. Zhang and W. Liu, *Dalton Trans.*, 2018, DOI: 10.1039/C8DT03182G.

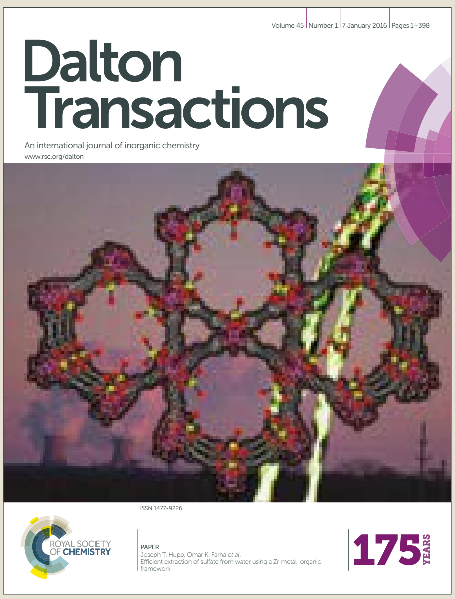

This is an Accepted Manuscript, which has been through the Royal Society of Chemistry peer review process and has been accepted for publication.

Accepted Manuscripts are published online shortly after acceptance, before technical editing, formatting and proof reading. Using this free service, authors can make their results available to the community, in citable form, before we publish the edited article. We will replace this Accepted Manuscript with the edited and formatted Advance Article as soon as it is available.

You can find more information about Accepted Manuscripts in the author guidelines.

Please note that technical editing may introduce minor changes to the text and/or graphics, which may alter content. The journal's standard Terms & Conditions and the ethical guidelines, outlined in our author and reviewer resource centre, still apply. In no event shall the Royal Society of Chemistry be held responsible for any errors or omissions in this Accepted Manuscript or any consequences arising from the use of any information it contains.

ROYAL SOCIETY OF CHEMISTRY

rsc.li/dalton

Please do not adjust margins

View Article Online
DOI: 10.1039/C8DT03182G

Journal Name

ARTICLE

A family of mixed-lanthanide metal-organic frameworks thermometer in a wide temperature range

Received 00th January 20xx,
Accepted 00th January 20xx

DOI: 10.1039/x0xx00000x

www.rsc.org/

Yang Yang, Haipeng Huang, Yingzhe Wang, Fangzhou Qiu, Yan Feng, Xuerui Song, Xiaoliang Tang, Guolin Zhang and Weisheng Liu*

By choosing 2-pyridin-4-yl-4,5-imidazoledicarboxylic acid (H_3PIDC) as the first ligand and sodium oxalate (OX) as the ancillary ligand, a series of mixed-lanthanide metal-organic frameworks (M'LnMOFs) $[Tb_{1-x}Eu_x(HPIDC)(ox)_{1/2}H_2O]\cdot 3H_2O$ (x= 0 **1**,0.01 **2a**, 0.03 **2b**, 0.05 **2c**, 0.08 **2d**, 0.1 **2e**, 0.3 **2f**, 0.5 **2g**, 1 **3**) have been successfully synthesized via hydrothermal reactions. **2a-2f** can serve as ratiometric luminescent sensor for detecting temperature. In this co-doped system, **2d** shows excellent linear relationship response to temperature from 303 to 473 K and exhibits a maximum relative sensitivity (S_r) of 0.60% K^{-1} at 473 K. Furthermore, Powder X-ray diffraction (PXRD) experiments indicate that **2d** has excellent chemical stability under simulated physiological conditions and alkali-acid solutions with pH ranging from 4 to 11, which makes it possible to be applied in the physiological environment.

1. Introduction

Due to the advantages of porosity, adjustability of structure and size, as well as excellent thermal stability and chemical stability, metal-organic frameworks (MOFs) have been considered as one of the potential and multifunctional materials for practical application. In the past two decades, MOFs have been widely research in energy gas storage/separation,[1] catalysis,[2] optics,[3-5] electronics,[6,7] magnetism[8] and biomedicine.[9] Rare earth has excellent electrical, magnetic and optical properties. Among the research of rare earth materials, luminescence performance is the most extensive and important content and its emission range can cover from ultraviolet to near-infrared area (300~1550 nm).[10] Lanthanide metal-organic frameworks (Ln-MOFs) were constructed by the combination of the intrinsic spectroscopic properties of lanthanide ions and the designability of MOFs and they have unique characteristics such as long luminescence lifetimes, large Stokes shift, characteristic emissions and wide emission range. Based on the above advantages, Ln-MOFs can be widely used in white LEDs, ion detection, small molecule detection, explosive detection, pH detection and temperature sensing.[11-18]

Temperature plays a critical role in scientific research and people's daily life. It is an important parameter which needs to be accurate measured in materials science, biomedicine, energy science and many other fields.[19,20] Compared with the conventional contact-thermometers, luminescence-based thermometers have attracted much attention due to the noninvasiveness, accuracy, high spatial resolution, and feasibility to work in strong electromagnetic environment and fast-moving objects.[21-26] Early luminescent thermometers for measuring temperature rely on the luminescent intensity of single transition, and their accuracy are susceptible by external factors, such as optical occlusion, sensor material concentration, excitation power, and the environment-induced nonradiative relaxation. Due to overcoming the above defects, ratiometric luminescent thermometers have gradually become a hot research in the past few years, which using the intensity ratio of two independent emissions (e.g., Eu^{3+}/Tb^{3+}, Nd^{3+}/Yb^{3+}) as the ratiometric thermometric parameter. In 2012, Qian's group developed the first ratiometric luminescent MOF thermometer, $[(Eu_{0.0069}Tb_{0.9931})_2(DMBDC)_3(H_2O)_4]_3DMF_3H_2O$, which was based on the temperature-dependent luminescence of the $^5D_0\rightarrow{}^7F_2$ transition of Eu^{3+} at 615 nm and the $^5D_4\rightarrow{}^7F_5$ transition of Tb^{3+} at 546 nm. Lian et al. reported the first near-infrared Ln-MOF thermometer, $Nd_{0.577}Yb_{0.423}BDC\text{-}F_4$, which was based on the intensity ratio between emissions of Yb^{3+} at 980 nm and Nd^{3+} at 1060 nm.[21,22] Although these above-mentioned thermometers show application prospects to some extent, they still have some shortcomings to restrict the development of luminescent thermometer, such as low sensitivity, cryogenic and narrow application temperature range.[27,29,30] In addition, pH-stability

[a] a.Key Laboratory of Nonferrous Metals Chemistry and Resources Utilization of Gansu Province and State Key Laboratory of Applied Organic Chemistry, College of Chemistry and Chemical Engineering, Lanzhou University, Lanzhou 730000, P. R. China
[b] * Corresponding authors. Tel: +86 931 8915151; fax: +86 931 8912582
[c] .E-mail addresses: liuws@lzu.edu.cn (W. S. Liu)
Electronic Supplementary Information (ESI) available: [details of any supplementary information available should be included here]. See DOI: 10.1039/x0xx00000x

Published on 03 September 2018. Downloaded on 9/4/2018 1:12:51 AM.

Dalton Transactions Accepted Manuscript

Please do not adjust margins

View Article Online
DOI: 10.1039/C8DT03182G

Published on 03 September 2018. Downloaded on 9/4/2018 1:12:51 AM.

is also a significant factor restricting the development of luminescent thermometers. Unfortunately, most of the MOF materials that have been reported are usually unstable under acid-based solution, which limits their application in physiological environment. Therefore, a luminescent MOF thermometer with high chemical stability in a wide pH range is needed.

To obtain fresh Ln-MOFs that can work in a wide pH range, we focused on a dicarboxylic acid, H_3PIDC, to construct isomorphic Ln-MOFs. The imidazole structure can act as a buffer solution to maintain the structure of Ln-MOFs without damage, which is readily protonated/deprotonated in acidic or basic conditions. Based on many rewarding influences, the introduction of ancillary ligands into Ln-MOFs results in a significant increase of luminescent intensity.[31-33]

By choosing sodium oxalate (OX) as the ancillary ligand, a family of M'LnMOFs **2a-2g** has been successfully synthesized via hydrothermal reactions. The temperature-dependent photoluminescence properties indicate that **2a-2g** can be used as luminescent thermometers, of which **2d** shows good linear relationship response to a relatively wide temperature scope from 303 to 473 K and exhibits an excellent S_r of 0.60% K^{-1} at 473 K. With **2d** as the representative, the article systematically elaborates the properties and application potential of **2a-2f** to be used as luminescent thermometers.

2. Experimental section

2.1. Instruments and measurements

All chemicals were obtained commercially. ^1H and ^{13}C NMR spectra were measured on a JEOLBCS 400M spectrometer with tetramethylsilane (TMS, 0.00 ppm) as an internal standard. Mass spectral measurements (ESI) were performed on an LQC system (Finnigan MAT, USA). Fourier transform infrared (FT-IR) spectra were recorded on a Burker VERTEX 70 spectrometer using KBr discs. Elemental analyses (C, H, N) were recorded on a Vario EL elemental analyzer. The TGA analyses were measured on a Netzsch STA 449 F3 Jupiter apparatus under an N_2 atmosphere. PXRD data were collected in the 2θ = 5-50° range using a PANalytical X'Pert Pro diffractometer with CuKα radiation.

2.2. Synthesis of H_3PIDC

As shown in scheme S1, the ligand H_3PIDC was obtained according to the reported article.[34] O-Phenylenediamine (1.1 g) and isonicotinic acid (1.23 g) were poured into PPA (13 mL), and the reaction was performed at 448 K for 4-5 h. Then the solution was poured into cold water (60 mL). Ammonia (25~28%) was added slowly and the pH value was adjusted to 7-8. Subsequently, a large amount of white precipitate was produced. After stirring for 15 min, the mixture was filtered, washed with water and dried to give 2-(4-Pyridyl) benzimidazole (2) (1.63 g, yield: 88%).^1H NMR (400 MHz, DMSO-d_6) δ 13.28 (s, 1H), 8.78 (d, J = 6.1 Hz, 2H), 8.11 (d, J = 6.1 Hz, 2H), 7.69 (d, J = 48.0 Hz, 2H), 7.29 (s, 2H). ^{13}C NMR (100 MHz, DMSO-d_6) δ 151.02, 149.29, 137.64, 123.40, 122.13, 56.57, 19.07. ESI-MS m/z: Calcd. For $C_{12}H_9N_3$ 195.08, Found: 196.08 $[M+H]^+$.

2 (5 g) was dissolved in 98% H_2SO_4 (10.0 ml), 30% H_2O_2 (50.0 ml) was added dropwise and the resulted mixture was stirred at 383 K. Then the solution gradually heated (388-393-403-413 K) and reacted at 413 K for 1 h. The solution was cooled naturally and poured into ice water (200 mL), stirred, filtered and washed to give H_3PIDC as a pale yellow solid powder (5.38 g, yield: 80%). ^1H NMR (400 MHz, DMSO-d_6) δ 8.91 (d, J = 6.6 Hz, 2H), 8.52 (d, J = 6.7 Hz, 2H). ESI-MS m/z: Calcd. For $C_{10}H_7N_3O_4$ 233.04, Found: 144.04$[M\text{-}2CO_2\text{-}H]^-$, 188$[M\text{-}CO_2\text{-}H]^-$, 232.02 $[M\text{-}H]^-$.

2.3. Synthesis of 1, 3 and 2a-2g.

The crystal was synthesized according to the literature procedure.[35] Taking **1** as an example, H_3PIDC (0.25 mmol, 58 mg), $Tb(NO_3)_3$ (0.2 mmol, 69 mg), sodium oxalate (0.2 mmol, 24 mg), and H_2O (6 mL) were sealed into a reactor (23 mL) and heated at 433 K for four days. Then the mixture was cooled naturally and yellow block crystals were obtained by filtration and washed with ethanol. Yield: 50.0%. Calcd (%) for $C_{11}H_{11}N_3O_9Tb$ (488.15): C, 27.07; H, 2.27; N, 8.61; found: C, 26.07; H, 2.38; N, 8.76. IR (KBr, cm^{-1}): 3449(m), 3203(w), 1600(s), 1440(s), 1363(s), 1265(m), 1122(m), 985(m), 864(m), 792(s), 740(m), 665(m), 538(m). The CCDC number for **1** is 842720. The Tb/Eu mixed MOFs **2a-2g** were obtained similarly to **1**, except using $Tb(NO_3)_3{\cdot}6H_2O$ and $Eu(NO_3)_3{\cdot}6H_2O$ as starting materials. The molar ratios of Tb/Eu salts in **2a-2g** products were showed in Table S1. The yields of **2a-2g** were also showed in Table S1.

2.4. Luminescence measurements

The temperature measurements (320-473 K) were recorded on a high-temperature powder detection accessory. Room-temperature excitation and emission spectra for the samples were measured on a Hitachi F-7000 spectrofluorometer, with a photomultiplier tube voltage of 700 V; a scan speed of 1200 nm/s; and slit widths of 1.0 and 5.0 nm.

3. Results and discussion

3.1. Structural Description

Yellow block crystals were successfully synthesized via hydrothermal reactions, and they are isomorphic and exhibit the same network. Taking **1** as an example, X-ray single crystal diffraction analysis demonstrates that **1** crystallizes in the monoclinic space group $P2_{1/c}$. As described in literature 35, the asymmetric unit of **1** contains one crystallographically independent Tb^{3+} ion, a $HPIDC^{2-}$ ligand, half of an oxalate ligand, and three water molecules. The Tb^{3+} ion is coordinate to one N atom from imidazole ring and seven oxygen atoms. Four oxygen atoms comes from $HPIDC^{2-}$ ligand, two oxygen atoms comes from oxalate ligand and the last oxygen atom comes from the water molecule (Figure 1a). Two adjacent Tb^{3+} ions are connected by $HPIDC^{2-}$ ligands and assembled into the $[Tb_2]$ units, which further expanded into 1D chain

Dalton Transactions Accepted Manuscript

This journal is © The Royal Society of Chemistry 20xx

Please do not adjust margins
View Article Online
DOI: 10.1039/C8DT03182G

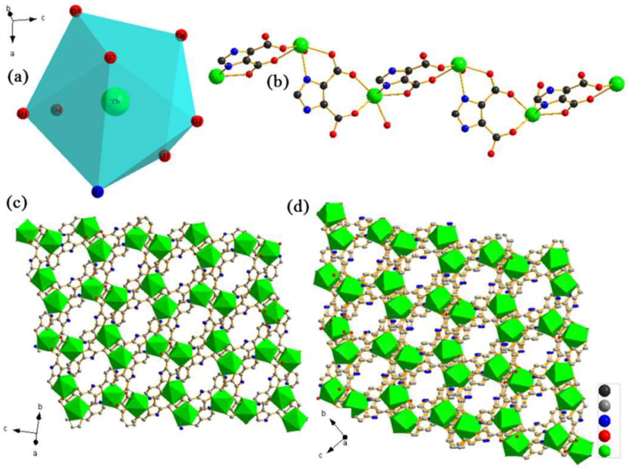

Figure 1. (a) Coordination environment of Tb^{3+}. (b) 1D Tb_2 chain motif showing the coordination polyhedral of the Tb atoms. (c) Perspective view of the 2D framework. (d) View of the 3D framework.

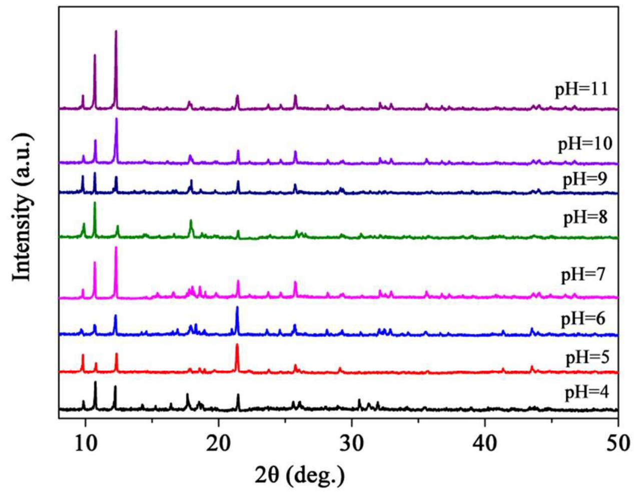

Figure 3. Power XRD of **2d** after being immersed in the solutions of pH= 4-11 for three days.

–Tb–O–C–O–Tb– geometrical patterns (Figure 1b). The adjacent 1D chain geometrical patterns are extended into the 2D metal–organic layers by the second coordination site of $HPIDC^{2-}$ ligands (Figure 1c). A 3D metal-organic framework is generated by adjacent layers (Figure 1d). The final coordination polyhedral of Tb^{3+} can be best described as a bicapped trigonal prism. PXRD experiments indicate that the M'LnMOFs is isostructural to the reported **1** (Figure 2).

3.2. Framework Stability

Stability is a limiting factor in the practical application of MOFs material, and high thermal stability is the primary condition to fabricate luminescent thermometers with a wide temperature range. The TGA analyses demonstrate that **2d** has high thermal stability with a decomposition temperature approximately high up to 400 °C, which is attributed to the tight 3D polymeric structure (Figure S1 and S2).

To further determine the potential applications of **2d**, the acid-base stability was also conducted. The solid powder of **2d** was successively immersed in the solutions of pH= 4-11 for three days, then separated by filtration and dried. The Powder XRD spectra of **2d** in solutions of pH = 4-11 shows slight changes, suggesting that **2d** has excellent stability in wide pH range (Figure 3). Encouraged by the outstanding pH stability, the luminescent spectrum of **2d** in solution of different pH was studied. The powder sample of **2d** was immersed in a 5 mL solution of different pH and ultrasonicated for 30 min to form emulsion, and then the luminescent spectrum was performed. The luminescent spectrum was in good agreement with PXRD, indicating that **2d** has excellent thermal and acid-base stability (Figure S3).

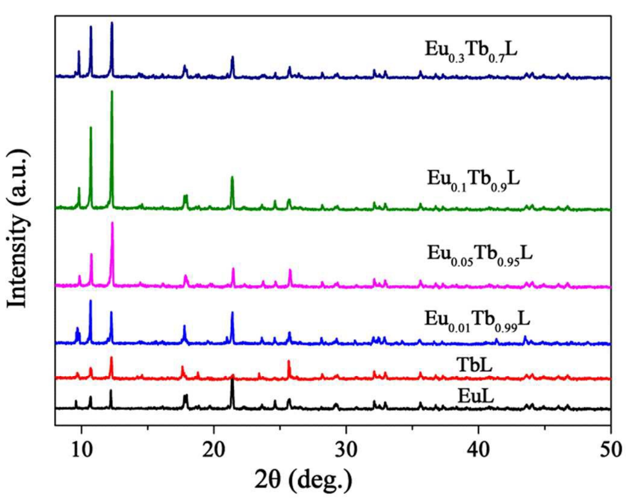

Figure 2. Powder XRD patterns of **1**, **3** and **2a-2g**.

3.3. Temperature-Dependent Photoluminescent Properties

Because of they are almost insoluble in most solvents such as DMSO, CH_3CN, DMF, EtOH, THF, MeOH, and H_2O, powder samples of **2a-2g** were used for all tests. The excitation and emission spectra of ligand H_3PIDC, **1**, **3** and **2a-2g** were investigated (Figure 4). The ligand of H_3PIDC exhibits a broad emission band at 408 nm under 422 nm excitation, which is presumably belong to the $\pi\rightarrow\pi^*$ transitions (Figure S4). Upon excitation at 333 nm, **1** and **3** exhibit the characteristic Tb^{3+} and Eu^{3+} emission bands, respectively, with a dominating intensity at 549 nm ($^5D_4\rightarrow{}^7F_5$) and 618 nm ($^5D_0\rightarrow{}^7F_2$) (Figure S5). As we expected, **2a-2g** simultaneously exhibit the typical Eu^{3+} (618 nm) and Tb^{3+} (549 nm) emission, implying efficient energy transfer from ligand H_3PIDC to the Eu^{3+} and Tb^{3+} ions (Figure S6-S8). Subsequently, the temperature-dependent photoluminescence properties of **1**, **3** and **2a-2g** were investigated from 320-473 K. As shown in Figure 5, luminescent intensities of Tb^{3+} and Eu^{3+} in **1** and **3** decreases drastically when the temperature increases, which is usually ascribed to the thermal activation of nonradiative-decay processes.[36-38] Although the non-radiative process produces a certain amount of heat, which doesn't affect the temperature of the sample in the process of measurement. Therefore, the

Published on 03 September 2018. Downloaded on 9/4/2018 1:12:51 AM.
Dalton Transactions Accepted Manuscript

Please do not adjust margins

View Article Online
DOI: 10.1039/C8DT03182G

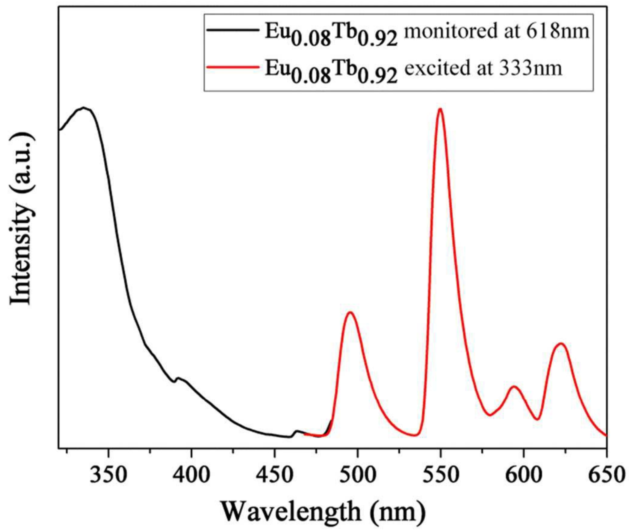

Figure 4. Excitation and emission spectra of **2d** at room temperature.

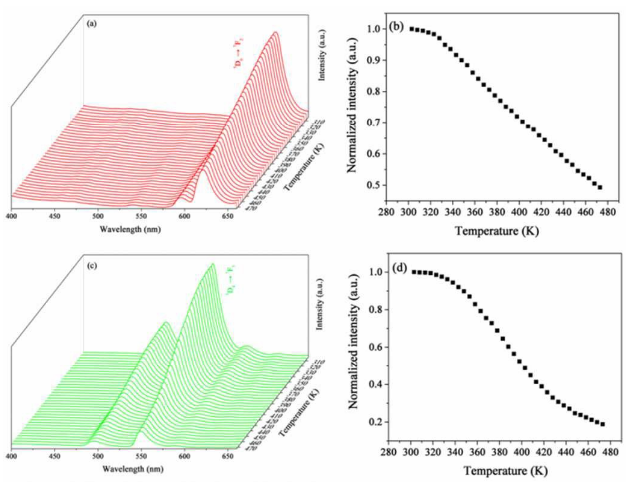

Figure 5. Emission spectra of (a) **3** and (c) **1** recorded between 303 and 473 K excited at 333 nm. Normalized emission intensities of (b) $^5D_0 \rightarrow ^7F_4$ transition of Eu^{3+} (618 nm) and (d) $^5D_4 \rightarrow ^7F_5$ transition of Tb^{3+} (549 nm).

non-radiative process will not have an impact on the temperature-dependent photoluminescence tests. As shown in Figure 6a, although the luminescent intensities of both Tb^{3+} and Eu^{3+} in **2d** decrease when the temperature increases, the luminescent intensity of Tb^{3+} reduces at a faster rate and the Eu^{3+} reduces at a slower rate compared with **1** and **3** (Figure 6b). When the temperature is 473 K, the intensity of Eu^{3+} occupies most of the spectrum. The same phenomenon was also observed in other materials, which is due to the energy transfer from the Tb^{3+} to Eu^{3+}.

We choose the intensity ratio of Tb^{3+} (549 nm) to Eu^{3+} (618 nm) (I_{Tb}/I_{Eu}) as the parameter in the temperature sensing process. The advantage of choosing this parameter is being a self-alignment dimension of the temperature from the luminescent intensity. The intensity ratio of **2d** as a function of temperature shows a good linear relationship in the range from 303 to 473 K that can be fitted as a function of

$$\Delta = 1.91473 - 0.00299T \qquad (1)$$

with a correlation coefficient (R^2) of 0.999, where T is the given temperature of **2d**, demonstrating **2d** is an excellent luminescent thermometer in relatively wide temperature scope from 303 to 473 K (Figure 6c). In order to further evaluate the performance of **2d**, the sensitivity was calculated according to equation (2) and (3), which is an important parameter for thermometer applications. The absolute sensitivity (S_{ab}) of luminescent thermometers can be defined as the change in the intensity ratio with temperature, as shown in equation (2):[39]

$$S_{ab} = \frac{\partial \Delta}{\partial T} \qquad (2)$$

and the relative sensitivity (S_r), which is usually more significative for practical applications, can be defined as in equation (3):[40]

$$S_r = \frac{(\partial \Delta / \partial T)}{\Delta} \qquad (3)$$

where Δ represents the I_{Tb}/I_{Eu} and T represents the temperature. According to the equation (2), the S_{ab} of **2d** is 0.003 K^{-1}. The S_r of **2d** increases gradually from 303 to 473 K, and reaches its maximum values of 0.6 % K^{-1} at 473 K (Figure 6d). The value of S_r is 4.3 times larger than that of the M'LnMOF luminescent thermometer $Tb_{0.99}Eu_{0.01}(BDC)_{1.5}(H_2O)_2$ reported by Carlos and 1.6 times larger than that of the first M'LnMOF ratiometric luminescent thermometer $Eu_{0.0069}Tb_{0.9931}$-DMBDC reported by Cui.[27,41] Compared to previously reported M'LnMOF luminescent thermometers, although the S_r of **2d** is not very prominent, a thermometer with a wide temperature range from 303 to 473 K is extremely rare (Table. 1). Furthermore, as shown in Figure 7, the samples **2d** of different batches basically show the same temperature-dependent photoluminescence emission spectrum and exhibit the same sensitivity of 0.6 % K^{-1} at 473 K. The temperature-dependent photoluminescence emission spectra of other M'LnMOF were also performed to evaluate the influences of

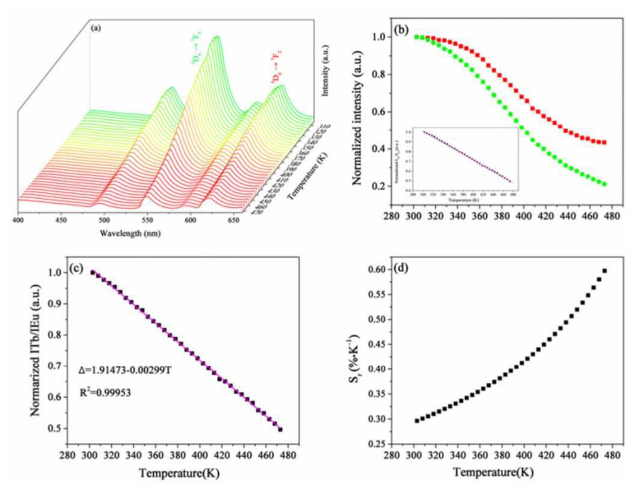

Figure 6. (a) Emission spectra of **2d** recorded between 303 and 473 K excited at 333 nm. (b) The normalized intensities of Eu^{3+}/618 nm (red) and Tb^{3+}/549 nm(green) in 2d; inset: the calibrated intensities of I_{Tb}/I_{Eu}. (c) Temperature-dependent normalized intensity ratio of Eu^{3+} (618 nm) to Tb^{3+} (549 nm) and the fitted curve for **2d**. (d) Temperature-dependent relative sensitivity (S_r) of **2d**.

Published on 03 September 2018. Downloaded on 9/4/2018 1:12:51 AM.
Dalton Transactions Accepted Manuscript

This journal is © The Royal Society of Chemistry 20xx

Please do not adjust margins
View Article Online
DOI: 10.1039/C8DT03182G

Published on 03 September 2018. Downloaded on 9/4/2018 1:12:51 AM.
Dalton Transactions Accepted Manuscript

Table 1. Composition, working ranges (K), maximum relative sensitivity values (Sm, % K^{-1}), and the temperature at which S_m is maximum (T_m, K) of ratiometric luminescent MOF thermometers.

Luminescent MOF	Range (K)	S_m (% K^{-1})	T_m
$Tb_{0.92}Eu_{0.08}$-HPIDC-OX	**303-473**	**0.6**	**473**
$Eu_{0.0069}Tb_{0.9931}$-DMBDC [14]	50 - 200	1.15	200
$Tb_{0.99}Eu_{0.01}(BDC)_{1.5}\cdot(H_2O)_2$ [28]	290-320	0.31	318
$Tb_{0.9}Eu_{0.1}$PIA [29]	100-300	3.27	300
$[Eu_{0.7}Tb_{0.3}(cam)(Himdc)_2(H_2O)_2]_3$ [30]	100-450	0.11	450
ZJU-88⊃perylene [31]	293-353	1.28	293
Eu^{3+}0.5%/Tb^{3+}99.5%@In(OH)(bpydc) [32]	283-333	2.53	333
$Tb_{0.957}Eu_{0.043}$cpda [27]	40-300	16	300
$Tb_{0.98}Eu_{0.02}(OA)_{0.5}(DSTP)\cdot 3H_2O$ [33]	77-275	2.4	275
$Eu_{0.0878}Tb_{0.9122}$L [34]	75-250	4.9	250
$Tb_{0.80}Eu_{0.20}$BPDA [17]	298-318	1.19	313
$Eu_{0.2}$ $Tb_{0.8}$ L [35]	40-300	0.15	300
$\{[Eu_2(L)_3\cdot(H_2O)_2\cdot(DMF)_2]\cdot 16H_2O\}_n$ [16]	10-150	0.12	150

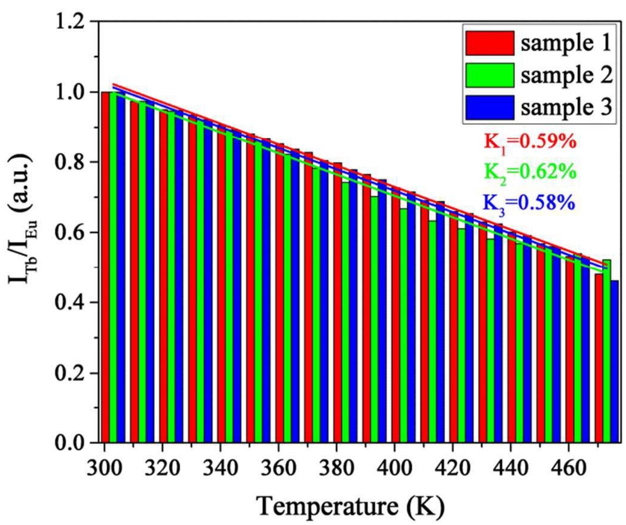

Figure 7. Temperature dependent intensity ratio of Tb^{3+} (549 nm) to Eu^{3+} (618 nm) in different batches of **2d** samples recorded between 303 and 473 K.

different proportions of Eu^{3+} and Tb^{3+}, suggesting that other M'LnMOF also have potential applications in temperature sensing (Figure S9-S15). Therefore, a better performance luminescent thermometer could be acquired by adjust the ratio of Eu^{3+} and Tb^{3+}.

In addition, the temperature-dependent photoluminescence emission spectrum of **2d** is illustrated by Commission Internationale de L'Eclairage (CIE) chromaticity diagram coordinates (Figure S16). The color of **2d** can slowly change from yellow to red, as the corresponding CIE coordinates change from (0.37, 0.4532) at 303 K to (0.3273, 0.3165) at 473 K, which can be expressly noticed by naked eye and camcorder. The CIE chromaticity diagrams of other thermometers are shown in Figure S17-S22. Therefore, **2d** can be used as a sensitive luminescent colorimetric thermometer in relatively wide temperature scope from 303 to 473 K.

3.4. Energy Transfer Mechanism

In the M'LnMOFs system, the mechanism of temperature-dependent luminescent responses has been clearly and systematically elucidated by the previous researchers, which is due to a typical process of energy transfer from one rare earth ion to another.[27,42-45] With the change of temperature, the process of energy transfer from one rare earth ion to another is the basis to design ratiometric luminescent thermometer. To further verify the mechanism of the energy transfer from Tb^{3+} to Eu^{3+}, the photoluminescence emission spectra of **2d** were carried out at room temperature upon excitation at 488 nm, which is belongs to the $^5D_4 \rightarrow {}^7F_6$ transition of the Tb^{3+} ion. As shown in Figure S23, the photoluminescence emission spectra of **2d** exhibits the characteristic Eu^{3+} emission bands at 618 nm ($^5D_0 \rightarrow {}^7F_2$ transition) and Tb^{3+} emission bands at 549 nm ($^5D_4 \rightarrow {}^7F_5$ transition), respectively. The results fully illustrate that the process of energy transfer from Tb^{3+} to Eu^{3+} actually happened. Similarly, the mechanism has also been proved by the photoluminescence emission spectra of other M'LnMOF at room temperature upon excitation at 488 nm (Figure S24-S29).

3.5. MTT and Biocompatibility Assay

To assess the potential of **2d** in biological applications, the stability and toxicity was preliminarily investigated under simulated physiological conditions. We immersed the solid powder of **2d** in the phosphate buffered saline (PBS) solutions for 24 h, filtered and dried naturally to give sample powder, followed by XRD experiment. The XRD profile shows slight changes, suggesting that **2d** has excellent stability under simulated physiological conditions (Figure 8). Furthermore, the cytotoxicity of **2d** was performed by MTT assay. Baby hamster kidney (BHK) cells were selected as the model and seeded in a 12-well culture plates. A various concentrations of **2d** (0, 10, 20, 50, 100 and 200 μg/mL) were added to the wells and incubated for 48 h. As shown in Figure S30, the cells still maintain high viability (＞95%) after incubation with high concentration (200 μg/mL) of **2d**, which suggests that **2d** has no obvious toxicity to living cells. The results clearly

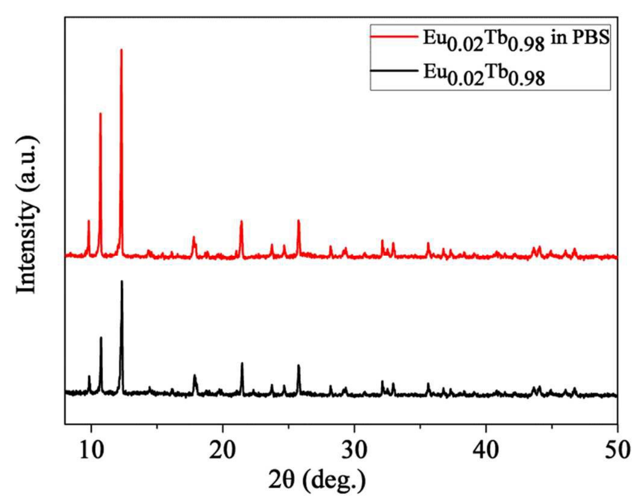

Figure 8. PXRD patterns of **2d** and **2d** immersed in PBS solution for 24 h.

Please do not adjust margins

View Article Online
DOI: 10.1039/C8DT03182G

demonstrate that **2d** has a low toxicity and good biocompatibility.

4. Conclusions

Temperature plays an important role in many intracellular chemical reactions and physiological processes, such as cell division, gene expression, and enzyme reaction. Therefore, a series of ratiometric luminescent thermometers were synthesized and they have excellent stability in wide pH range from 4 to 11. Compared with pure inorganic or organic thermometers, which are based on gold-CdTe nanoparticles, quantum dot clusters, organic dye molecule, rare-earth doped materials and NIPAM materials,[46-48] the ratiometric luminescent thermometers is generally concerned by the researchers as an organic-inorganic hybrid materials due to the accuracy, noninvasiveness, and the ability to work in fast-moving objects and strong electromagnetic environment. Preliminary studies prove that **2d** has excellent stability, low toxicity and good biocompatibility under simulated physiological conditions. Furthermore, based on the signal-to-noise ratios of spectrometer, the theoretical temperature sensing resolution of **2d** is found to be 0.012 K,[30] which is accurate enough to monitor the tiny temperature change of pathological and normal cells.[49] Therefore, we believe that **2d** can be used as a practical temperature sensing materials for the disease diagnosis in the near future.

Conflicts of interest

There are no conflicts to declare.

Acknowledgements

This work was supported by the National Natural Science Foundation of China (Grants 21431002).

References

1 R. Easterday, O. Sanchez-Felix, Y. Losovyj, M. Pink, B. D. Stein, D. G. Morgan, M. Rakitin, V. Y. Doluda, M. G. Sulman, W. E. Mahmoud, A. A. Al-Ghamdi and L. M. Bronstein, *Catal. Sci., Technol*., 2015, **5**, 1902.
2 Y. A. Kabachii, A. S. Golub, S. Y. Kochev, N. D. Lenenko, S. S. Abramchuk, M. Y. Antipin, P. M. Valetsky, B. D. Stein, W. E. Mahmoud, A. A. Al-Ghamdi and L. M. Bronstein, *Chem. Mater*., 2013, **25**, 2434.
3 Y. Cui, Y. Yue, G. Qian and B. Chen, *Chem. Rev*., 2012, **112**, 1126.
4 M. D. Allendorf, C. A. Bauer, R. K. Bhakta and R. J. T. Houk, *Chem. Soc. Rev*., 2009, **38**, 1330.
5 J. Rocha, L. D. Carlos, F. A. A. Paz and D. Ananias, *Chem. Soc. Rev*., 2011, **40**, 926.
6 W. E. Mahmoud, *Sens. Actuators. B*., 2017, **238**, 1001.
7 Z. Hu, B. J. Deibert and J. Li, *Chem. Soc. Rev*., 2014, **43**, 5815.
8 W. E. Mahmoud, *Mater. Lett*., 2016, **177**, 42.
9 A. Bétard and R. A. Fischer, *Chem. Rev*., 2012, **112**, 1055.
10 K. Binnemans, *Chem. Rev*., 2009, **109**, 4283.
11 L. E. Kreno, K. Leong, O. K. Farha, M. Allendorf, R. P. Van Duyne and J. T. Hupp, *Chem. Rev*., 2012, **112**, 1105.
12 Z. Yu-Cheng, Z. Liang, L. Hong-Yan, X. Qiu-Lei, T. Ming-Yu, Z. You-Xuan, Z. Jing-Lin, Z. Hong-Jie and Y. Xiao-Zeng, *Adv. Mater*., 2011, **23**, 4041.
13 R. Mojgan, Z. Xiao and L. Jing, *Angew. Chem*., 2012, **124**, 451.
14 F. Luo, M.-S. Wang, M.-B. Luo, G.-M. Sun, Y.-M. Song, P.-X. Li and G.-C. Guo, *Chem. Commun*., 2012, **48**, 5989.
15 J. Della Rocca, D. Liu and W. Lin, *Accounts. Chem. Res*., 2011, **44**, 957.
16 J.-P. Zhao, J. Xu, S.-D. Han, Q.-L. Wang and X.-H. Bu., *Adv. Mater*., 2017, **29**, 1606966.
17 H. Wang, J. Xu, D.-S. Zhang, Q. Chen, R.-M. Wen, Z. Chang and X.-H. Bu., *Angew. Chem. Int. Edit*., 2015, **54**, 5966.
18 Q. Gao, J. Xu, D. Cao, Z. Chang and X.-H. Bu., *Angew. Chem. Int. Edit*., 2016, **55**, 15027.
19 W. Zhuopeng, A. Duarte, C.-S. Arnau, B. C. D. S., I. Inhar, M. Daniel, R. João and C. L. D., *Adv. Funct. Mater*., 2015, **25**, 2824.
20 Y. Zhou and B. Yan, *J. Mater. Chem. C*., 2015, **3**, 9353.
21 S. Uchiyama, A. Prasanna de Silva and K. Iwai, *J. Chem.Educ*., 2006, **83**, 720.
22 F. Jiao, T. Kaijun, H. Dehui, W. Shuangqing, L. Shayu, Z. Yi, L. Yi and Y. Guoqiang, *Angew. Chem*., 2011, **123**, 8222.
23 C. D. S. Brites, P. P. Lima, N. J. O. Silva, A. Millán, V. S. Amaral, F. Palacio and L. D. Carlos, *New. J. Chem*., 2011, **35**, 1177.
24 X. Meng, S.-Y. Song, X.-Z. Song, M. Zhu, S.-N. Zhao, L.-L. Wu and H.-J. Zhang., *Inorg. Chem. Front*., 2014, **1**, 757.
25 S.-N. Zhao, X.-Z. Song, M. Zhu, X. Meng, L.-L. Wu, J. Feng, S.-Y. Song and H.-J. Zhang, *Chem – Eur. J*., 2015, **21**, 9748.
26 M. Zhu, X. Z. Song, S. Y. Song, S. N. Zhao, X. Meng, L. L. Wu, C. Wang and H. J. Zhang., *Adv. Sci*., 2015, **2**, 1500012.
27 Y. Cui, H. Xu, Y. Yue, Z. Guo, J. Yu, Z. Chen, J. Gao, Y. Yang, G. Qian and B. Chen, *J. Am. Chem. Soc*., 2012, **134**, 3979.
28 X. Lian, D. Zhao, Y. Cui, Y. Yang and G. Qian, *Chem. Commun*., 2015, **51**, 17676.
29 D. Wang, Q. Tan, J. Liu and Z. Liu, *Dalton. T*., 2016, **45**, 18450.
30 D. Zhao, X. Rao, J. Yu, Y. Cui, Y. Yang and G. Qian, *Inorg. Chem*., 2015, **54**, 11193.
31 Y. Wei, Q. Li, R. Sa and K. Wu, *Chem. Commun*., 2014, **50**, 1820.
32 A. Fratini, G. Richards, E. Larder and S. Swavey, *Inorg. Chem*., 2008, **47**, 1030.
33 S. V. Eliseeva, D. N. Pleshkov, K. A. Lyssenko, L. S. Lepnev, J.-C. G. Bünzli and N. P. Kuzmina, *Inorg. Chem*., 2010, **49**, 9300.
34 S. Ting, M. Jian-Ping, H. Ru-Qi and D. Yu-Bin, *Acta. Crystallogr. E*., 2006, **62**, o2751.
35 S. Lin, L. Gui-Zhu, X. Mei-Hua, L. Xiao-Jian, L. Jian-Rong and D. Hong, Eur. J. *Inorg. Chem*., 2012, **2012**, 1764.
36 M. L. Bhaumik. *J. Chem.Phys*., 1964, **40**, 3711.
37 P. Hongshang, S. M. I. J., Y. Jiangbo, S. Li-ning, F. L. H. and W. O. S., *Adv. Mater*., 2010, **22**, 716.
38 S. I. Weissman. *J. Chem.Phys*., 1942, **10**, 214.
39 E. J. McLaurin, L. R. Bradshaw and D. R. Gamelin, *Chem. Mater*., 2013, **25**, 1283.
40 Y. Cui, W. Zou, R. Song, J. Yu, W. Zhang, Y. Yang and G. Qian, *Chem.Commun*., 2014, **50**, 719.
41 A. Cadiau, C. D. S. Brites, P. M. F. J. Costa, R. A. S. Ferreira, J. Rocha and L. D. Carlos, *ACS. Nano*., 2013, **7**, 7213.
42 X. Rao, T. Song, J. Gao, Y. Cui, Y. Yang, C. Wu, B. Chen and G. Qian, *J. Am. Chem. Soc*., 2013, **135**, 15559.
43 Y.-H. Han, C.-B. Tian, Q.-H. Li and S.-W. Du, *J.Mater. Chem. C*., 2014, **2**, 8065.
44 Y. Yang, L. Chen, F. Jiang, M. Yu, X. Wan, B. Zhang and M. Hong, *J. Mater. Chem. C*., 2017, **5**, 1981.
45 Z. Shu-Na, L. Lei-Jiao, S. Xue-Zhi, Z. Min, H. Zhao-Min, M. Xing, W. Lan-Lan, F. Jing, S. Shu-Yan, W. Cheng and Z. Hong-Jie, *Adv. Funct. Mater*., 2015, **25**, 1463.

Published on 03 September 2018. Downloaded on 9/4/2018 1:12:51 AM.
Dalton Transactions Accepted Manuscript

Please do not adjust margins
View Article Online
DOI: 10.1039/C8DT03182G

46 F. Ye, C. Wu, Y. Jin, Y.-H. Chan, X. Zhang and D. T. Chiu, *J. Am. Chem. Soc*., 2011, **133**, 8146.
47 C. Wu, B. Bull, C. Szymanski, K. Christensen and J. McNeill, *ACS. Nano*., 2008, **2**, 2415.
48 C. Wu, T. Schneider, M. Zeigler, J. Yu, P. G. Schiro, D. R. Burnham, J. D. McNeill and D. T. Chiu, *J. Am.Chem. Soc*., 2010, **132**, 15410.
49 B. Kateb, V. Yamamoto, C. Yu, W. Grundfest and J. P. *Gruen, NeuroImage*., 2009, **47**, T154.

Published on 03 September 2018. Downloaded on 9/4/2018 1:12:51 AM.

Dalton Transactions Accepted Manuscript

This journal is © The Royal Society of Chemistry 20xx

Please do not adjust margins

View Article Online
DOI: 10.1039/C8DT03182G

Published on 03 September 2018. Downloaded on 9/4/2018 1:12:51 AM.

Dalton Transactions Accepted Manuscript

Table of Contents

A family of mixed-lanthanide metal-organic frameworks thermometer in a wide temperature range.